BIODIVERSITAS
Volume 25, Number 7, July 2024
Pages: 2980-2992

ISSN: 1412-033X
E-ISSN: 2085-4722
DOI: 10.13057/biodiv/d250719

Biodegradability and formulation of triclosan-degrading and plant-growth-promoting *Pseudomonas* sp. MS45

MERRY KRISDAWATI SIPAHUTAR♥

Program of Occupational Health and Safety, Faculty of Vocation, Universitas Balikpapan. Jl. Pupuk Raya Gn. Bahagia Balikpapan, Balikpapan 76114, East Kalimantan, Indonesia. Tel: +62-542-765442, Fax: +62-542-764205, ♥email: merryksipahutar@yahoo.com; merry.k@uniba-bpn.ac.id

Manuscript received: 27 March 2024. Revision accepted: 9 July 2024.

Abstract. *Sipahutar MK. 2024. Biodegradability and formulation of triclosan-degrading and plant-growth-promoting* Pseudomonas *sp. MS45. Biodiversitas 25: 2980-2992.* This study presents the isolation of *Pseudomonas* sp. MS45, a microorganism that can consume triclosan (TCS) as its only carbon and energy source, leading to its detoxification. The rarity of a toxicity study of TCS before and after biodegradation treatment is addressed in this study. *Allium cepa*'s genotoxicity exposed TCS's cytotoxicity, generating multiple damaged chromosomes, in contrast to the insignificant consequences of its broken-down metabolites. The study also optimized the different kinetic parameters for TCS-specific biodegradation and *Pseudomonas* sp. MS45-specific growth. The biodegradation pattern followed the Michaelis-Menten model with a maximum specific biodegradation rate (Vmax) of 0.01 µmole h-1 mg cell protein-1 and a half saturation constant (Ks) of 21.98 µM. The growth pattern followed the Haldane model with a maximum specific growth rate (µmax) of 0.03 h-1, half saturation constant (Ks) of 4.56 µM, and TCS inhibition constant (Ki) of 32.81 µM. In addition to its TCS-degrading ability, *Pseudomonas* sp. MS45 also possesses various plant growth promotion traits, and it was incorporated into two solid carrier formulations: vermiculite and rice bran. The study found that vermiculite, especially with PEG, was the most consistent formulation for *Pseudomonas* sp. MS45, in terms of maintaining bacterial survival and TCS-degrading ability. This study marks the initial report on the biodegradation and formulation of TCS-destroying and Plant-Growth-Promoting (PGP) *Pseudomonas* sp. MS45, offering promising implications for environmental and agricultural applications.

Keywords: Formulation, plant-growth-promoting, *Pseudomonas* sp. MS45, toxicity, triclosan

INTRODUCTION

Triclosan (TCS), an antiseptic employed in pharmaceutical and personal care goods, has proven very hazardous to numerous organisms (Nandikes et al. 2022; Jayalatha and Devatha 2023). There is ample evidence that TCS can be biodegraded to methyl triclosan, 2,4-dichlorophenol, and 2,8-dichlorodibenzoparadioxin, which are also assumed as harmful or persistent chemicals (Contardo-Jara et al. 2021; Suthar et al. 2023). Due to its chemical stability, persistence, and toxicological impacts on living organisms, even at low concentrations, it has been designated as one of the primary important contaminants and is receiving attention. TCS is dangerous for human health since it can disrupt hormones and have an adverse effect on many tissues. It also has been demonstrated to negatively affect aquatic creatures, including fish, algae, and invertebrates (Olaniyan et al. 2016); hence, the US EPA registered TCS as a pesticide (Taştan et al. 2017). Consequently, developing a highly efficient method for removing TCS and its compounds from polluted environments is significant. Photocatalytic degradation and sophisticated oxidation processes have been employed for the chemical treatment of TCS.

To date, TCS has been broken down or transformed by physico-chemical processes such as sorption, adsorption, photocatalyzed mineralization, and electrochemical oxidation (Granatto et al. 2021; Araújo et al. 2022; Nie et al. 2022). However, these treatments are expensive and have intrinsic disadvantages, such as producing more poisonous and recalcitrant intermediates. Thus, a great concern in biological treatment has been exposed to be a successful substitute due to its high efficiency, high selectivity, affordability, and environmental friendliness. Microbial treatments are being investigated to degrade TCS using *Providencia rettgeri* MB-IIT (Balakrishnan and Mohan 2021); *B. megaterium* Y-4 (Chen et al. 2022); *Thauera* (Dai et al. 2022b); microbial community (Dong et al. 2021); *Pseudomonas* strain (Devatha and Pavithra 2019); bacterial strains (Aguilar-Romero et al. 2020); microalgae-bacteria consortia (Chan et al. 2022); *Pleurotus ostreatus* and *Trametes versicolor* (Mallak et al. 2020); and the Sphingomonadaceae family (Cui et al. 2022; Dai et al 2022a). However, studies on the capacity of these bacteria to degrade metabolites produced during the TCS transformation are scarce. Moreover, towards sustainable and green bioremediation technologies, the utilization of Plant-Growth-Promoting Bacteria (PGPB) to degrade toxic compounds in the agricultural field should be emphasized because it can provide an efficient, economic, and sustainable green remediation technology for the recent century environment (Sharma et al. 2022a). Using pollutant-degrading PGPB in agricultural areas can reduce soil toxicity and stimulate plant growth. Previous research has shown that soil contaminants can negatively impact PGPB growth and their ability to promote plant growth. Therefore, it is crucial to use

bacteria that can thrive even in toxic environments (Vocciante et al. 2022).

However, applying inoculant to soils may face difficulties because, generally speaking, the bacterial population gradually decreases soon after being added to the soil (Satapute et al. 2019; Schlatter et al. 2022; Qu et al. 2023). Therefore, to overcome this problem, it is necessary to develop a well-formulated bacteria that can raise the likelihood that they will perform at their best and achieve financial success in farming production (Araujo et al. 2020; Sharma et al. 2022b; Singh and Arora 2023).

The way forward is the extensive screening of microorganisms to obtain a vigorous culture, which can degrade TCS aerobically and detoxify it rapidly under the prevailing conditions. *Pseudomonas* sp. is the most extensively analyzed to degrade a very wide range of aromatic pollutants (Qi et al. 2022; Phulpoto et al. 2022). In this investigation, *Pseudomonas* sp. MS45 was isolated from pesticide-contaminated sites and used for the degradation and detoxification of TCS. The parameters kinetics of biodegradation and bacterial growth were determined to signify that *Pseudomonas* sp. MS45 can efficiently decompose TCS at high doses; further, plant-growth-promoting features of *Pseudomonas* sp. MS45 was also determined in the present study; finally, the formulation of *Pseudomonas* sp. MS45 was developed to demonstrate its capability and shelf life during storage for bioremediation potential. As far as we are aware, this is the initial report revealing the biodegradability and formulation of *Pseudomonas* sp. MS45 that degrades TCS.

MATERIALS AND METHODS

Chemicals and culture medium

TCS was acquired from Tokyo Chemical Industry Co., Ltd., in Tokyo, Japan. Over 96% of TCS was pure. We obtained acetone from J.T. Baker (manufactured in the USA). The other substances were all analytically graded. The TCS degradation test was conducted using growing cells of a bacterial strain in Mineral Salts Medium (MSM), pH 6.8-7, which contained 5.8g Na_2HPO_4; 3.0g KH_2PO_4; 0.5g NaCl; 0.25g $MgSO_4$; and 1.0g NH_4Cl per liter of deionized water (Satapute et al. 2019). The bacterial formulation was prepared using Mineral Salts Medium Yeast (MSMY), pH 6.8-7, with 5.8g Na_2HPO_4, 3.0g KH_2PO_4, 0.5g NaCl, 0.25g $MgSO_4$, 1.0g NH_4Cl, and 5.0g yeast for every one liter of deionized water. Then, it was mixed with 20 g L^{-1} agar to generate the solid medium. The medium was disinfected by autoclaving at 121°C for 20 min.

Isolation and identification of pure strain

Utilizing pesticide-contaminated soil samples, bacteria that could break down TCS were isolated through an enrichment culture approach. Soil samples were taken from a lengthy bean cultivation field in Thailand. Enriching TCS-degrading bacteria involved adding 5 g of the obtained soil sample into 100 mL of MSM. TCS (40 µM, or 11.58 mg L-1) was introduced to MSM as the only energy source and carbon. Next, using an orbital rotary shaker set at 120 rpm, the flasks underwent a two-day incubation at 28±2°C. A 0.2 mL portion was put into MSM agar plates with 40 µM of TCS as the carbon and energy source. Colonies that remained viable after two days of incubation at 30°C were chosen from the plates to determine their TCS resistance.

A pure strain of bacteria with the greatest capacity for TCS biodegradation and cell growth was subsequently identified by partial 16S rDNA sequencing (Pan et al. 2021). A generic primer set for bacteria was utilized for Polymerase Chain Reaction (PCR) amplification. The set included the forward primer (27f: 5'-AGA GTT TGA TCS TGG CTC AG-3') and the reverse primer (1492r: 5'-GGT TAC CTT GTT ACG ACTT-3'). These were the PCR conditions: 30 cycles of 95°C (30 s), 57°C (30 s), 72°C (1.5 min), and a final 10 min-chain extension cycle at 72°C. The pre-denaturation step was conducted at 94°C for 3 min. Following purification, the amplicons were sequenced. The NCBI's BLAST search was performed on the sequences to identify closely related sequences. Mega software (version 6) generated a phylogenetic tree, which was then joined using the neighborhood approach. The confidence estimates for the phylogenetic tree topologies were computed with a bootstrap value of 1,000.

Growth and TCS degradation

Aerobic condition

Cell cultures were grown in 5 mL of LB liquid media with continuous 120 rpm trembling and harvested in every experiment after the log phase. These cultures were employed as starters. The starters were injected at 8% (v:v) into 100 mL MSM with 40 µM TCS, then submerged in a rotary shaker set to 120 rpm at 28±2°C. The experiment was performed under growth-dependent conditions. TCS's standard solution (in acetone, 100 mM was liquefied) was poured into the 250 mL flasks, and before adding the MSM media, the acetone was allowed to evaporate. As abiotic controls, inoculation cultures were generated using the same methodology as previously described. The degradation tests were carried out in an aerobic environment. After giving each solution flask a good shake, each flask was kept at room temperature. A culture sample was taken at predetermined times to measure cell growth and residual TCS using a spectrophotometer to measure cell optical density at 600 nm. After taking 1 mL of solution out of each vial and centrifuging for 10 minutes at 10,000 rpm to extract the cells, the degradation of TCS was assessed. The TCS residues in the supernatant were assessed using HPLC (LC-20AT, Shimadzu) with the following specifications: mobile phase: acetonitrile: UP water (70:30), temperature of column: 40°C, wavelength: 254 nm, flow rate: 1 mL/min, and injection volume: 20 µL. Next, compare the peak regions of the common compounds and the unknown peaks allowed for the acquisition of quantitative data.

Anaerobic condition

Biodegradation tests under anaerobic conditions were carried out under various external electron acceptors and external donors in 150 mL serum bottles under growth dependent experiment. Fresh sterile MSM medium (90 mL)

and 8% (v:v) culture inoculum were added to each serum bottle. Serum bottles were flushed with pure nitrogen gas and enclosed with aluminum covers and a butyl rubber stopper (Franke et al. 2020). TCS was added to all culture samples at a starting 40 µM concentration. To study the influence of external electron acceptor on TCS degradation, 20 µM of ferric, sulfate, and nitrate was added to the cultured medium (Chen et al. 2024). To study the influence of external electron donors on TCS degradation, 1g/L of succinic acid, glucose, and acetate was added to the cultured medium (Sun et al. 2023). An anaerobic control experiment containing no electron acceptor or electron donor and no cell culture was run in parallel. All solution serum bottles were vigorously shaken and incubated at 120 rpm at room temperature. The remaining TCS was measured by taking culture samples at pre-arranged intervals. Furthermore, the liquids underwent a 10-minute centrifugation at 10,000 rpm to extract the cells. The HPLC (LC-20AT, Shimadzu) was used to examine the TCS residues in the supernatant under the following parameters: 40°C column temperature, 254 nm wavelength, 1 mL/min flow rate, acetonitrile: UP water (70:30) mobile phase, and 20µL volume of injection. Quantitative information was derived by contrasting the unknown compounds' peak height with the reference compounds. Additionally, TCS had a 6.189±0.013 minute retention time under these analytical circumstances.

LC/MS analysis of metabolites formed during biodegradation

Numerical data was acquired by contrasting the peak areas of the conventional compounds and unknown peaks; the biodegradation intermediate(s) produced during the transformation of TCS by *Pseudomonas* sp. MS45 were identified by HPLC and examined using a Liquid Chromatograph/Mass Spectrometer (LC/MS) fitted with a microtof-Q II 10335 Series Electrospray Ionization (ESI) source.

Growth and biodegradation kinetic analysis

The kinetic studies conducted in an aerobic environment followed the previously described protocol, with TCS concentrations ranging from 5 to 60 µM. The concentration of residual TCS and absorbance at 600 nm were determined at different intervals. Next, the precise growth rate and exact degradation rate were identified. Data on a particular growth rate and substrate concentration were fitted employing the Haldane substrate inhibition model. The TCS concentrations and the specific biodegradation rate were then plotted using the Michaelis-Menten model to estimate the degradation kinetic. GraphPad Prism 5 was used to solve the model equations, and Microsoft Excel®'s data analysis toolkit was utilized to analyze regression. All kinetic experiments were conducted in triplicate.

Cytogenotoxicity assessment of TCS and its degraded metabolites

A prior study showed that the cytogenotoxicity experiment was conducted on meristematic cell tips at the roots of a healthy *Allium cepa* (Kumar et al. 2022). Thus, using a fine razor blade, onion bulbs were carefully stripped of their desiccated roots and outside scales to prevent harming the meristematic tissues. The bulbs were kept dark for three days while submerged with newly distilled water to avoid drying out the primordial cells. Every day, distilled water was replaced. In brief, *A. cepa* fresh root tips were exposed to varying doses (0, 40, and 80 µM) of TCS, extracted using acetone, and its degradation metabolites were submitted to an aerobic 4-hour experiment. A negative control was applied by treating the root tips with distilled water. Thus, the root tip was steeped in 1 N HCl for 10 min, cleaned with purified water, then incubated for 90 min in glacial acetic acid and 95% ethanol mixture. On a microscopic slide, the crushed root tips were dyed with 1% aceto-orcein after being immersed in 45% acetic acid. Cell division and chromosomal aberration of the tagged root tips were seen using microscopy at 1000× magnification. The percentage difference between the number of cells scored overall and the division of cells (1050) was designated as the mitotic index.

Determination of plant-growth-promoting potential of *Pseudomonas* sp. MS45

The traits of plant-growth-promoting (phosphate solubilization, organic acid, Indole Acetic Acid (IAA), Exo-Polysaccharides (EPS), siderophore, production of ammonia) of *Pseudomonas* sp MS45 was studied in two concentrations of TCS (40 and 80 µM). Treatment without TCS was performed as a control.

Bioassay for phosphate solubilization (P-solubilization)

P-solubilization was ascertained by modifying Pacwa's technique (Pacwa et al. 2016). After adding 0, 40, and 80 µM of TCS to 100 mL of Pikovskaya broth, 1 mL of 10^8 cells/mL was used to inoculate each strain of bacteria. The flasks were shaken at 120 rpm for seven days at 28±2°C. Each flask containing 20 mL of culture broth was taken out and centrifuged at 10,000 rpm for 30 minutes. Briefly, chemicals for color reactions were synthesized in the following manner: 0.5 M trichloroacetic acid and 0.1 M ascorbic acid are present in Reagent A. After dissolving ascorbic acid (0.704 g) and trichloroacetic acid (3.268 g) in 10 mL of water, the amount was increased to 40 mL. The reagent B is ammonium molybdate (0.01 M). After being dissolved in 100 mL of water, 2.472 g of ammonium molybdate was added to make 200 mL capacity. Five percent acetic acid, 2 mg of sodium arsenite, and 1 mg of sodium citrate comprise Reagent C (hazardous). Next, glacial acetic acid (10 mL) was added to the 100 mL of dissolved sodium citrate and sodium arsenite. We then changed the volume to 200 mL. Reagent A should be added to 0.40 mL to 0.32 mL of samples. A mixture was created by adding reagent B (0.08 mL) first, then reagent C (0.20 mL). The changing shade of blue was discovered Using a spectrophotometer set to 600 nm. The KH_2PO_4 calibration curve at 0, 20, 40, 60, 80, and 100 µg mL^{-1} was utilized to ascertain the total amount of P-solubilized (He and Honeycutt 2005). Additionally, the shift of pH upon tricalcium phosphate solubilization was detected.

Bioassay for organic acids production

The qualitative and quantitative synthesis of organic acids was verified using an HPLC Shimadzu Japan system outfitted with a C-18 column and UV detector. In the mobile phase, 50 mM KH_2PO_4 was added at a 0.7 mL/min flow rate. Absorbance at 210 nm was used to detect organic acids. They were found and measured by comparing the retention periods and peak areas to solutions of pure acids (Fitriatin et al. 2022).

Bioassay for Indole Acetic Acid (IAA) production

Pacwa's method was used to quantitatively analyze Indole Acetic Acid (IAA) (Pacwa et al. 2016). In short, the bacterial strain was cultured in an LB medium (pH 7). After being infected with 1 mL of a 10^8 cells mL^{-1} bacterial strain, 100 mL of LB broth containing 100 µg L-tryptophan mL^{-1} was shaken (120 g) for 24 hours at 28±2°C. Next, TCS at 0, 40, and 80 µM concentrations was added to the broth. Following the incubation period, 10 minutes were spent centrifuging 5 mL of every culture at 10,000 rpm. After adding ofex 2 mL of Salkowsky-reagent to supernatant (2 mL), the mixture was left to sit at 28°C in the dark for 1 hour. A spectrophotometer at 540 nm was used to measure the amount of IAA in the supernatant according to a conventional curve of 0, 20, 40, 60, 80, and 100 µg/mL.

Bioassay for Exo-Polysaccharides (EPS) production

Bacteria were cultured in 100 mL of basal media containing 5% sucrose and added to 0, 40, and 80 µM concentrations of TCS. The strains were then shaken (at 120 rpm) for four days at 28±2°C to produce Exo-Polysaccharides (EPS). After 30 minutes of spinning the culture broth at 5,000 rpm, 1 mL of supernatant and 3 mL of cooled acetone were added to extract the EPS. Following an overnight drying period, the precipitated EPS was rinsed thrice consecutively with distilled water and acetone, and the pellets were weighed (Pacwa et al. 2016).

Bioassay for siderophore production

Siderophore production was evaluated quantitatively by employing the Modi medium according to the method of Pacwa and freinds (Pacwa et al. 2016). A 100 mL Modi medium subjected with 0, 40, 80 µM concentration of TCS was incubated at 28±2°C for five days after being infected with 100 µL of 107 cells mL^{-1} of bacterial cells. The centrifugation of the cultures at 5,000 rpm allowed for the measurement of the catechol-type phenolates in the liquid culture, specifically Salicylic Acid (SA) and 2,3-Dihydroxybenzoic Acid (DHBA), using a modified version of Hathway's ferric chloride-ferricyanide reagent (Reeves et al. 1983). Shortly, 2 mL of supernatant was extricated twice with 2 mL of ethyl acetate at pH 2 to create ethyl acetate extracts. Hathway's reagent was made by mixing 100 µL of 0.1 M potassium ferricyanide and 100 µL of 0.1 M ferric chloride in 0.1 N HCl with 100 mL of distilled water. In the experiment, 1 mL reagent was mixed with 1 mL sample. The absorbance was measured at 700 nm for dihydroxy phenols using DHBA as the standard and at 560 nm for Salicylates (SA) using sodium salicylate as the standard. SA and DHBA calibration curves were run at 0, 20, 40, 60, 80, and 100 µg mL^{-1}.

Bioassay for ammonia production

Moreover, bacterial cells were cultured in peptone water broth for five days at 28±2°C to perform the ammonia test. Next, 200 µL culture was combined with 1 mL of the Nessler reagent, and the assortment's volume was raised to 8.5 mL by adding distilled water free of ammonia. The transition of color from brown to yellow signifies the formation of ammonia. The spectrophotometer measured the amount of ammonia in the solution at 450 nm (Goswami et al. 2014). Next, using the ammonium sulfate standard curve, the ammonia content was determined to be 0, 0.10, 0.25, 0.50, 0.75, 1.00, and 1.25 mg mL^{-1}.

Formulation of strain MS45

The formulation of *Pseudomonas* sp. MS45 was determined in two-based carriers, including vermiculite and rice bran. Stock liquid pure culture of strain MS45 was prepared in Minimum Salt Mineral Yeast (MSMY) medium supplemented with benzoic acid 100 ppm in a conical flask and then kept at 28±2°C for 24 hours at 120 rpm in a rotary shaker; the concentration reached around 1010 CFU/mL. Various types of polymer additives (1%, w/w) were added to the solid formulations; these are Polyethylene Glycol (PEG), Polyvinyl Pyrrolidone (PVP), mixed of (50-50%) Carboxymethyl Cellulose (CMC) and glycerol, and gum arabic. A 1% (v/w) molasses (as a nutrient) and 100 ppm of benzoic acid (to inhibit all wild strains) were also supplemented to each formulation. All materials except carriers were separately autoclaved at 15 psi pressure at 121°C for 20 min. Both vermiculite and rice bran (150 g) were filled separately in autoclavable polypropylene bags and autoclaved thrice at 15 psi pressure at 121°C for 20 min three days a row. Additive singly, 1% molasses, 1% polymer additive, and 100 ppm benzoic acid were supplemented to each carrier (150 g) following a 24-hour oven drying process at 28±2°C to get the finished dried formulation (Silva et al. 2016). After that, 60 mL of stock culture was transferred to the mixture under an aseptic condition and shaken for uniform distribution. All the solid-based formulations with a moisture content of 40% were packed and sealed individually in polypropylene bags, with roughly 25% left open to allow for adequate aeration of the inoculants (McPherson et al. 2018). After that, the bags were kept for 20 weeks at 28±2°C in the dark to protect against heat and Ultraviolet (UV) ray damage (Maheshwari et al. 2015). Periodically, samples were collected to assess the cell viability in terms of CFU and the capacity of the cells to break down TCS. The bags were gently but thoroughly shaken before sampling to ensure that the inoculant was evenly distributed throughout the formulation. Next, 1 g was taken from each strain MS45 formulation and serially diluted with sterile water. In Petri plates (0.2 mL/plate), 1 mL suspension from 10^{-5} and 10^{-8} dilutions was placed over solidified MSMY plus 40 µM (or equivalent to 11.58 mg L^{-1}) TCS, and the dishes were incubated at 30°C for 24 hours. The MS45 colony development was measured and reported as log CFU/g of formulation product.

TCS degradation tests were conducted in an environment dependent on growing cells. 250 mL Erlenmeyer flasks

containing MSM medium (100 mL), 8% (w/v) solid formulation MS45, and TCS were added. 1 mL of the contents of each vial was removed, and the solutions were centrifuged for 10 minutes at 10,000 rpm to extract the cells and evaluate TCS degradation. As was previously indicated, TCS residues were analyzed in the supernatant using HPLC.

Statistical analysis

Three runs of each test were conducted with GraphPad Prism, version 5.03 (CA, USA). After that, the data were statistically assessed using Dunnett's multiple comparison test. A one-way ANOVA at a 5% probability threshold assessed the significant difference among treatment means.

RESULTS AND DISCUSSION

Isolation and identification of *Pseudomonas* sp. MS45

Pesticide-contaminated soil yielded a bacterial strain named MS45 that could use TCS as its only carbon and energy source. This strain was motile, non-spore, short, and rod-shaped, and it tested negative for Gram staining. MS45 was further identified by determining the 16S rDNA sequence. After being sequenced, a 16S rDNA segment with 1498 nucleotides was submitted for BLAST analysis to NCBI. Based on evolutionary distance measurements, the neighbor-joining technique was applied to obtain the phylogenetic position of the strain MS45, as illustrated in Figure 1. According to the alignment, MS45 had 99% sequence identity with *Pseudomonas* reactants PSR2 (GQ354529) and *Pseudomonas fluorescens* LMG5329 (LQ974027), indicating a close relationship. Based on these findings, strain MS45 was identified as a *Pseudomonas* species named *Pseudomonas* sp. MS45. *Pseudomonas* sp. has shown great promise in the bioremediation of several hazardous contaminants. Hexadecane, polyester polyurethane, crude oil, toluene, polycyclic aromatic hydrocarbon, formaldehyde, arsenate, catechol, chloroanilines, carbazole, and pyrene have all been documented to be degraded by some *Pseudomonas* sp. bacteria. However, only a small number of studies have found that *Pseudomonas* sp. degrades TCS to date (Shah et al. 2016; Devatha and Pavithra 2019; Thelusmond et al. 2019; Hajieghrari and Hejazi 2020). This work reports on a unique strain of *Pseudomonas* sp. for the first time. MS45 can degrade TCS and use it as its only carbon and energy source; this finding will expand the use of *Pseudomonas* sp. MS45 in developing plant growth under and without TCS stress circumstances (Hajieghrari and Hejazi 2020).

Bacterial growth, TCS degradation, and its transformation by *Pseudomonas* sp. MS45

Figure 2 depicts the development of *Pseudomonas* sp. MS45 in liquid MSM enhanced with 40 µM and its capacity to break down TCS. Without any lag phase, the growth curve demonstrated a strong increase in bacterial density. HPLC analysis revealed a significant drop in TCS concentrations simultaneously; *Pseudomonas* sp. MS45 decomposed approximately 57.5% of the 40 µM TCS given after 6 days of aerobic incubation; as a result, the cell densities increased from 0.073 to 0.182 of OD600; *Pseudomonas* sp. MS45 could not grow when it was put into a culture without the addition of TCS, and there was no discernible change in the concentration of TCS in cultures that were not infected with the bacterium. Thus, we deduced that TCS may be broken down and used as a carbon source by *Pseudomonas* sp. MS45.

Biopurification systems are designed to remove organic pollutants from wastewater using bacterial communities. However, other pollutants in such systems may impact the bacterial communities and affect the ecotoxicity results reported in previous studies. It is important to investigate how different pollutants interact with each other and how they affect the effectiveness of biopurification systems. Dissipation of ibuprofen, diclofenac, and TCS, alone and in mixes, in biopurification system microcosms, paying special emphasis to their effect on bacterial ecotoxicity and community structure and composition. Separately, biopurification systems use microcosms to disperse ibuprofen and diclofenac far more effectively than to remove TCS. Furthermore, the dissipation time was longer when a combination of ibuprofen, diclofenac, and TCS was applied to biopurification system microcosms. TCS exhibited an initial unfavorable effect on bacterial viability; however, this effect was alleviated when ibuprofen, diclofenac, and TCS were present simultaneously (Aguilar-Romero et al. 2020).

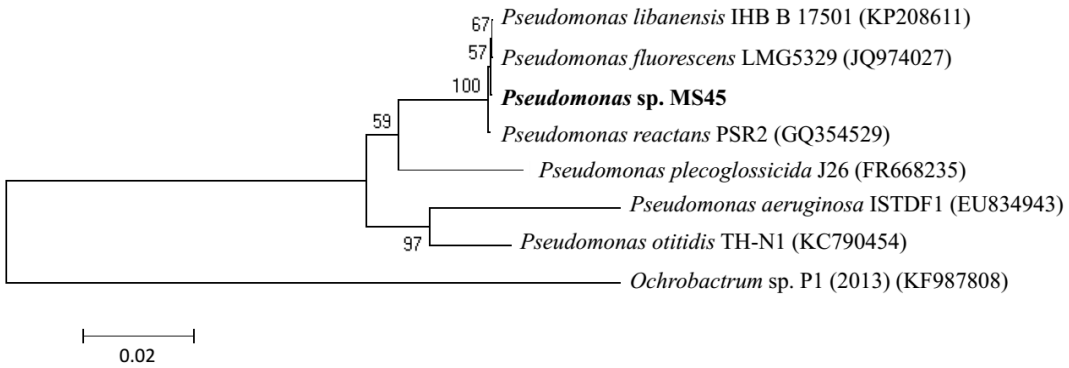

Figure 1. The phylogenetic tree of MS45 and related strains was constructed using the 16s rRNA gene sequences. Bootstrap values were calculated using 1000 replicas. The outgroup utilized was *Ochrobactrum* sp. P1 (2013) (KF987808)

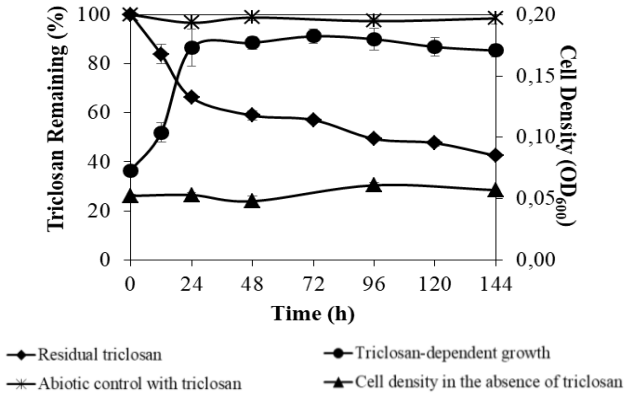

Figure 2. TCS deterioration and growth pattern of *Pseudomonas* sp. MS45 at 40 µM concentration under aerobic conditions

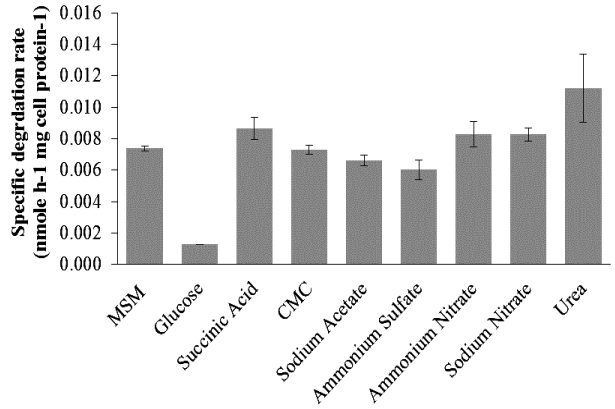

Figure 3. Impact of nitrogen and carbon supplementary on the specific degradation rate of TCS by *Pseudomonas* sp. MS45. A significance level of $p<0.05$ does not distinguish bars with identical lowercase letters

On the other hand, the degradation efficiency dramatically decreased in anaerobic conditions. During the 14-day incubation period, there was little biodegradation of TCS. TCS could not be degraded in control cultures grown in the same anaerobic conditions without an electron acceptor or donor. These findings suggest that, in anaerobic environments, this chemical survives and exhibits a high degree of resistance to biodegradation. The exact parameters that allowed TCS to remain in the anaerobic state are unknown (Nandikes et al. 2022).

Figure 3 presents the findings of biodegradation studies showing the impact of additional nitrogen and carbon sources; the specific degradation rate of TCS by *Pseudomonas* sp. MS45 in addition to carbon and nitrogen sources, mostly showed insignificant differences. The same phenomenon occurred to triclocarban degradation by *Ochrobactrum* sp. MC22 and *Pseudomonas fluorescens* MC46 (Sipahutar and Vangnai 2017; Sipahutar et al. 2018), and by adding urea, *Pseudomonas* sp. MS45 resulted in a slight increase in the specific degradation rate of TCS. On the contrary, the addition of glucose significantly declined the biodegradation efficiency of TCS, even though its supplementation to the medium greatly increased the bacterial density. A similar co-substrate, which exhibited similar results, has been used in 3,3′,4,4′-tetrachlorobiphenyl (PCB 77) degradation by *Sinorhizobium meliloti* NM (Wang et al. 2017). Glucose probably played as *Pseudomonas*'s carbon catabolite suppression not only prevented the breakdown of undesirable substances but also had the potential to cause a significant metabolic rearrangement that would have required the activation of several genes (Sun et al. 2018). To this point, *Pseudomonas* sp. MS45 prefers glucose as the first carbon and energy source more than TCS. Hence the same phenomenon, in addition to inorganic nitrogen (no significant effect) and organic carbon (slightly significant), occurs on *p*-nitrophenol (PNP) degradation by *Ochrobactrum* sp. B2 (Subba Reddy et al. 2016).

Based on HPLC analysis, only one metabolite was detected during the time-course biodegradation study. The peak height of metabolite increased proportionally to the decrease in the peak height of TCS. Further, the metabolite was detected as 2,4-Dichlorophenol (2,4-DCP; molecular ion m/z 163) by Mass Spectrometry analysis. 2,4-DCP was degradable by *Pseudomonas* sp. MS45 as well. The biodegradation kinetics of 2,4-DCP followed the Michaelis-Menten model with a maximum specific biodegradation rate (Vmax) of 0.007 µmole h-1 mg cell protein-1 and a half saturation constant (K_s) of 18.39 µM. The transformation of TCS to 2,4-DCP was not first reported in this study. It convinces the TCS biodegradation pathway proposed earlier (Li et al. 2015; Dou et al. 2018).

Previously reported, multiple intermediates were found during TCS degradation by bacterial communities in biopurification systems; the first degradation mostly included the hydroxylation of aromatic rings, followed by dechlorination. Using C-C bond cleavage and ether bond fission, intermediates were created, including 2-chlorohydroquinone, 4-chlorocatechol, and 4-chlorophenol. These compounds may then be further converted into unchlorinated compounds, which would finally lead to full stoichiometric free chloride release (Nandikes et al. 2024). However, bacterial communities influence the TCS biodegradation mechanism (Dai et al. 2020).

Kinetics of *Pseudomonas* MS45 growth and TCS biodegradation

Therefore, to determine the kinetics of the degradation process and the potential of a single culture of *Pseudomonas* sp. MS45 to degrade TCS, the batch experiment was conducted in 250 mL Erlenmeyer flasks with a working volume of 100 mL; the starting concentration of *Pseudomonas* sp. MS45 was adjusted from 5 to 60 µM in the MSM medium to evaluate the bacterial growth profile utilizing TCS as the substrate. A non-linear regression of the Haldane inhibition formula determined the specific growth rate (µ) at varying concentrations.

$$\mu = \frac{\mu_{max}\, S}{S + (S^2/K_i) + K_s}$$

Where:

µ : Specific growth rate (h^{-1})
μ_{max} : Maximum specific growth rate (h-1)
S : Various initial TCS concentrations (µM)
Ki : Inhibition constant (µM)
Ks : Half-saturation growth constant (µM)

The specific growth rate profile, which indicates a high degree of fit for the Haldane inhibition model with an R2 value of 0.96, is shown in Figure 4.A. The μ_{max} of *Pseudomonas* sp. MS45 was estimated to be 0.035 h^{-1}. With an estimated K_s value of 4.86 µM, or 1.41 mg L^{-1}, *Pseudomonas* sp. MS45 has a strong preference for this hazardous chemical. After a concentration of 10 µM, there was a slight decrease in the growth curve slope, and the K_i value was found to be 32.81 µM, or 9.49 mg L^{-1}. Nonetheless, the growth rate specific to bacteria stayed at 70% of its maximum value. This finding indicates that *Pseudomonas* sp. MS45 was able to withstand elevated TCS concentrations. As far as we know, this is the first work to present TCS biodegradation's bacterial growth kinetic characteristics.

The specific biodegradation kinetic was fitted to the Michaelis-Menten model to estimate kinetic parameters. Many studies have used a rate model of the Michaelis-Menten type to examine the kinetics of substrate conversion by enzymes or living cells (Holkar et al. 2014). The following represents the relationship between substrate concentration and specific biodegradation rate:

$$\frac{dS}{dt} = -V_{max}\frac{S}{S + K_s}$$

$$\frac{S}{v} = \frac{1}{Vmax}[S] + \frac{Ks}{Vmax}$$

Where:

Ks and Vmax: Half-saturation concentration (µM) and maximum specific biodegradation rate of TCS (µmole h^{-1} mg cell $protein^{-1}$), respectively.

The specific biodegradation rate profile is displayed in Figure 4.B. The following were the biodegradation kinetic parameters of this model: K_s = 21.98 µM (or 6.38 mg L^{-1}) and V_{max} = 0.012 µmole h^{-1} mg cell $protein^{-1}$ (or equal to 0.004 mg substrate h^{-1} mg cell $protein^{-1}$). According to the profile, the specific biodegradation rate increased as TCS concentration increased. This profile shows that microorganisms are not inhibited from degrading TCS up to a concentration of 60 µM. In contrast to the previously published TCS biodegradation kinetics of *Sphingopyxis* strain KCY1 (Dou et al. 2018), it may be inferred that K_s of the TCS biodegradation process by *Pseudomonas* sp. MS45 had a comparatively high value. Furthermore, this Ks value is significantly greater than the ambient concentrations of TCS in wastewater (0.61 to 5.1 mg L^{-1}) (Durán-Álvarez 2015), indicating TCS degradation by *Pseudomonas* sp. MS45 fits the first-order degradation kinetics in wastewater.

Cytogenotoxicity of TCS and its metabolites

As a good bioindex of the genotoxic, mutagenic effects, and cytotoxic of surroundings contaminated by noxious chemicals, the root tip cell assay using *A. cepa* has proven to be a delicate and quick tool for monitoring environmental toxicity (Scussel et al. 2022). The chromosomal aberration percentage, Mitotic Indexes (MI), and *A. cepa* meristematic cells exposed to TCS and its metabolites were identified. The MI value of *A. cepa* root tips was reduced from that in the non-toxic control (distilled water) by 43% and 52% in the presence of 40 and 80 µM TCS, respectively; however, biological treatment of TCS by *Pseudomonas* sp. MS45 enhanced the MI value of *A. cepa* root tips by 36% and 40% at 40 and 80 µM TCS, respectively (Table 1). The MI value, the total number of dividing cells in the cell cycle, has been used to evaluate the cytotoxicity of various contaminants. A decrease or increase in the MI value can indicate a pollutant's cytotoxicity levels (Yadav et al. 2019). The higher MI value in metabolite-degraded cells compared to TCS-treated cells indicates the harmless characteristics of the metabolites. The lower MI of *A. cepa* meristematic cells can be a reliable technique for measuring the cytotoxicity of TCS pollutants in the environment.

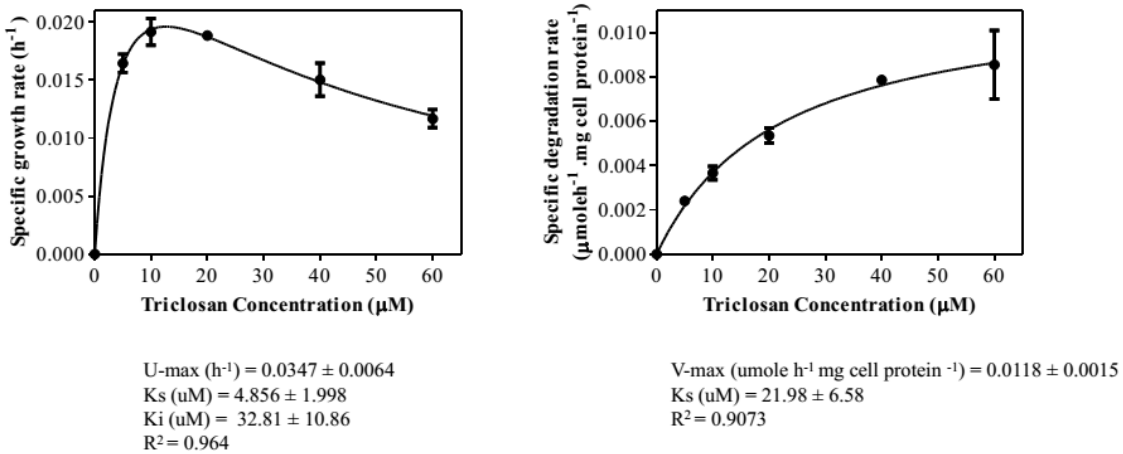

Figure 4. A. Haldane model-fitted TCS-dependent specific growth kinetics of *Pseudomonas* sp. MS45; B. Michaelis-Menten model-fitted connection between the specific biodegradation rate and TCS concentrations by *Pseudomonas* sp. MS45

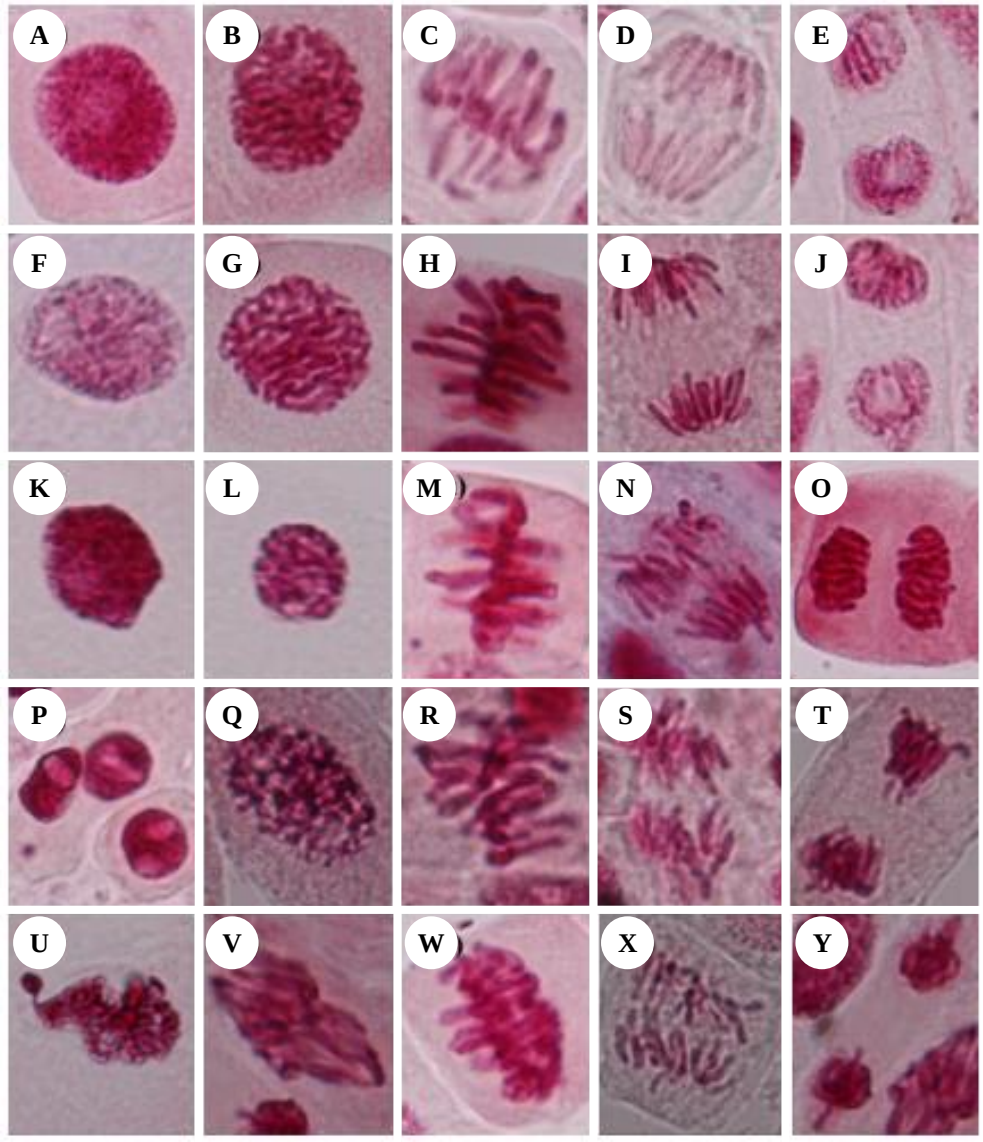

Figure 5. Cytogenotoxicity study of TCS and the metabolites that it breaks down in *A. cepa* meristematic cells. The following test solutions were applied to *A. cepa* root tips: (A-E) distilled water; (F-J) 40 µM degraded metabolites; (K-O) 80 µM degraded metabolites; (P-T) 40 µM TCS; (U-Y) 80 µM TCS. A. interphase; B. prophase; C. metaphase; D. anaphase; E. telophase; F. intrephase; G. prophase; H. metaphase; I. anaphase; J. telophase; K. prophase; L. prophase; M. abnormal metaphase; N. laggard anaphase; O. telophase; P. bi-nucleated cell at interphase; Q. prophase; R. laggard metaphase; S. multipolar anaphase; T. telophase with chromosome loss; U. apoptosis; V. disoriented chromosom at prophase; W. sticky metaphase; X. multipolar anaphase; Y. laggard telophase

In addition to MI, *A. cepa* treated with TCS, by-products, and pure water (as a non-toxic control) exhibited chromosomal abnormalities that were also characterized by changes in chromosomal structures (Figure 5) in chromosomal aberration index (percentage) and total number of chromosomes (Table 1). Meristematic cells exposed to distilled water, a non-toxic control, displayed normal physiology with minuscule aberrations of 0.1%. The highest chromosomal aberration index of 1.4 % was observed in 80 µM TCS-treated root cells. In TCS-exposed cells, anomalies like chromosome lagging, multipolar anaphase, chromosome loss, sticky chromosomes, and apoptosis chromosomes were noticed. However, cells of degraded metabolites showed insignificant chromosomal aberration throughout every stage of the *A. cepa* cell.

All of these data show that the isolated *Pseudomonas* sp. MS45 can not only degrade but also detoxify TCS. The same results were also reported on the cytogenotoxicity reduction of azo dye by *Serratia liquefaciens* and *Enterococcus gallinarum* (Soni et al. 2016; Haq et al. 2018) as well as 4-nitroaniline by *Acinetobacter* sp. AVLB2 (Silambarasan and Vangnai 2016).

Plant-growth-promoting traits of *Pseudomonas* sp. MS45

Plant-Growth-Promoting Bacteria (PGPB) can increase the growth of plants directly or indirectly, assist plants in withstanding contaminants, and enhance plant remediation capacities (Alves et al. 2022); *Pseudomonas* sp. MS45 was examined in vitro to see if it may express characteristics that Promote Plant Growth (PGP). It showed six PGP traits:

phosphate-solubilization, Exo-Polysaccharides (EPS), Indole Acetic Acid (IAA), siderophore, ammonia (NH3), and organic acid production. In the current investigation, *Pseudomonas* MS45 tolerated substantial amounts of TCS (40 and 80 µM) and possessed the tested PGP traits.

Increasing the availability of phosphorus in soil requires the release of phosphorus in its fixed and insoluble forms. (Sindhu et al. 2014). Utilizing phosphate-solubilizing bacteria as inoculants increases crop production and plant phosphorus uptake concurrently (Cruz et al. 2022). Bacteria that fall into categories of plant growth are reportedly aided by *Pseudomonas*, which solubilizes insoluble phosphate molecules (Blanco-Vargas et al. 2020). In the absence of TCS stress, *Pseudomonas* sp. MS45 showed the highest phosphate-solubilizing activity in this investigation. Furthermore, there is no discernible difference in the P-solubilization amount when the two TCS concentrations are present (Table 2). Formic acid and gluconic acid were produced during phosphate-solubilization in both the absence and presence of TCS (Table 1). These findings demonstrated no correlation between the amount of organic acids generated and the amount of phosphate-solubilized *Pseudomonas* MS45, with the most phosphate-solubilization resulting in the least total organic acids produced. *Streptomyces* sp. likewise reveals a similar outcome, in which there was no correlation between the amounts of solubilized phosphorous and the amounts of organic acids in the culture medium (Cui et al. 2022).

EPS secretion varies slightly depending on whether TCS is present or not, much like the phosphate-solubilization tendency of *Pseudomonas* MS45 does (Table 2). One important role of rhizobacteria is the synthesis of Extracellular Polymeric Substances (EPS), which shields the bacterial cell from phagocytosis and drying out and promotes the fixation of nitrogen by blocking high oxygen tension phage attacks (Naseem et al. 2018). Strain *Pseudomonas* MS45 produced IAA in both the presence and absence of TCS (Table 2). The two concentrations' impact of TCS tested did not vary on phytohormone IAA synthesized by *Pseudomonas* MS45. These results reveal that *Pseudomonas* MS45 could maintain the IAA production even under stress conditions. In plants, IAA produced by PGPB influences apical dominance, phototropism, geotropism, growth rate, root initiation, and cell division and enlargement (Olanrewaju et al. 2017). As a result, IAA is crucial for interactions between rhizobacteria and plants (Ma et al. 2022).

Furthermore, in the absence of TCS stress, *Pseudomonas* sp. MS45 showed the production of the maximum siderophore (SA and DHBA). There is no discernible difference between the amount of SA produced by *Pseudomonas* MS45 under TCS stress and normal circumstances. In contrast, the amount of DHBA steadily dropped as the TCS concentration rose. Despite the harmful chemical stress, 70% of reasonable activity was maintained (Table 2). The siderophores production indicates *Pseudomonas* sp. MS45 as a potential biocontrol against soil-borne phytopathogens. Because it is linked to nitrogen (N_2) fixation and is mostly seen in leguminous rhizobacteria, ammonia (NH_3) generation was considered a significant PGP feature. Legumes and nitrogen-fixing microbes have a symbiotic relationship responsible for the important biochemical events involved in biological N_2 fixation, transforming atmospheric elemental N_2 into NH_3 (Hirsch and Mauchline 2015). Plants interact with various PGPBs, considerably boosting plant development and yield (Singh et al. 2018). In this study, *Pseudomonas* sp. MS45 produced significant ammonia both with and without TCS presence, and the production activity was effectively sustained.

Therefore, to our knowledge, no such study has evaluated the impact of TCS on bacterial PGP characteristics. These findings demonstrate that *Pseudomonas* sp. MS45 can naturally display various PGP properties and suggest that the bacterium could be a useful bioinoculant for TCS bioremediation in agricultural fields contaminated with TCS.

Formulation of *Pseudomonas* sp. MS45

The cell viability and TCS-degrading ability of *Pseudomonas* sp. MS45 in the formulations was tested using low-cost carriers (vermiculite and rice bran) with polymer additives (Polyethylene Glycol (PEG), Polyvinyl Pyrrolidone (PVP), mixed of (50-50%) Carboxymethyl Cellulose (CMC) and glycerol, and gum arabic). The initial viability of *Pseudomonas* sp. MS45 in all the tested formulations ranged between 8.94 and 9.50 log CFU g^{-1} product. The application of vermiculite and rice bran, along with polymer additives, caused no inhibition of the growth of *Pseudomonas* sp. MS45. Vermiculite was found to be superior for the growth of *Pseudomonas* sp. MS45, when compared to the rice bran (Figure 6).

The cell viability of *Pseudomonas* sp. MS45 in vermiculite, with all polymer additives tested, was well maintained until 20 weeks of storage. In bioformulation preparation, the carrier is the main component that ensures that bioformulations are commercially successful by providing the proper number of living cells in a good physiological state at the appropriate time (Gopalakrishnan et al. 2016). Vermiculite has sufficient water-holding capacity, major natural moisture content, almost normal pH, and non-toxic qualities that allow for the growth of big microbial communities (Maheshwari et al. 2015).

Among different selected polymer additives, the greatest CFU count of *Pseudomonas* sp. MS45 after 20-week storage was recorded on PEG (9.20 log CFU g^{-1}) followed by PVP (8.59 log CFU g^{-1}). The most inferior formulation of *Pseudomonas* sp. MS45 was observed in rice bran with gum arabic, where the cell count of 9.25 log CFU g-1 initially decreased to 5.89 logs CFU g^{-1} after 20 weeks in storage (Figure 6). In the present study, the most optimum polymer additive for the formulation of *Pseudomonas* sp. MS45 in both vermiculite and rice bran was PEG. The number of log CFU of *Pseudomonas* sp. MS45 after 20 weeks of storage with PEG in vermiculite and rice bran was 9.20 log CFU g^{-1} and 7.71 log CFU g^{-1}, respectively. The mechanism of action of these additives is still not clear. However, it is supposed that the effect of PEG and PVP is modulated by altering the water activity of media and may also influence the movement of solutes in both the media and the cell membrane (Dayamani and Brahmaprakash 2014).

Table 1. The chromosomal aberration and mitotic indexes were measured in *A. cepa* root tip cells treated with control, TCS, and degraded metabolites

	Concentration of the compound (µM)	No. of dividing cells	Mitotic Index (MI) %	Aberration Index (AI)%	Chromosomal aberrations				
					ML	MC	MA	AL	CB
Distilled water (control)		191 a	18.2±0.93 a	0.1±0.03 c	0	0	0.63±0.31	0	0
TCS	40	108 d	10.4±0.23 d	1.2±0.22 a	3.03±0.86	0	2.27±0.34	4.35±0.72	2.61±0.41
	80	93 d	8.8±0.36 d	1.4±0.11 a	0	4.62±0.18	2.99±0.37	2.12±0.34	4.94±0.23
Degraded metabolites	40	148 b	14.1±0.52 b	0.4±0.05 b	1.99±0.14	0	0	0	2.18±0.42
	80	129 c	12.3±0.29 c	0.6±0.09 b	0	0	0	2.01±0.36	3.87±0.62

Note: The number of chromosomes per 1050 cells; the mitotic index, or MI%, is calculated as (dividing cells/total cells seen) × 100. MC stands for metaphase cluster, ML for metaphase lagging chromosome, AL for anaphase lagging chromosome, and CB for chromosomal breaks. Each value represents the mean ±SD of three replicates for every treatment. According to Dunnett's multiple comparison test, distinct letters within the same column indicate significant variations at $P<0.05$ compared to the control

Table 2. *Pseudomonas* sp. MS45 affects plant development at different concentrations of TCS

Treatments	Phosphate solubilized		EPS (µg mL^{-1})	IAA (µg mL^{-1})	Siderophores		Ammonia (µg mL^{-1})	Organic acid production	
	Liquid-based medium (µg mL^{-1})	pH			SA (µg mL^{-1})	DHBA (µg mL^{-1})		Gluconic acid (µg mL^{-1})	Formic acid (µg mL^{-1})
TCS (40 µM)	55.39±1.53 a	3.4	41.87±3.01 a	4.81±0.26 a	30.1±1.5 b	13.3±1.1 b	709.75±42.14 a	6.02±0.38 c	5.24±0.26 c
TCS (80 µM)	54.34±0.94 a	3.0	40.25±3.89 a	5.48±0.46 a	28.1±0.7 a	10.5±1.2 a	668.3±8.91 a	5.17±0.19 a	6.49±0.16 c
Control	57.16±3.09 a	3.4	39.5±2.83 a	5.93±0.26 a	30.8±0.6 b	15±1.3 b	718.92±33.5 a	4.9±0.16 a	3.83±0.48 a

Note: The following are abbreviations: DHBA: 2,3-Dihydroxy Benzoic Acid; SA: Salicylic Acid; IAA: Indole Acetic Acid; and EPS: Exo-Polysaccharides. Each value represents the mean ±SD of three replicates for every treatment. According to Dunnett's multiple comparison test, different letters in the same column indicate significant differences from the control group at $P<0.05$

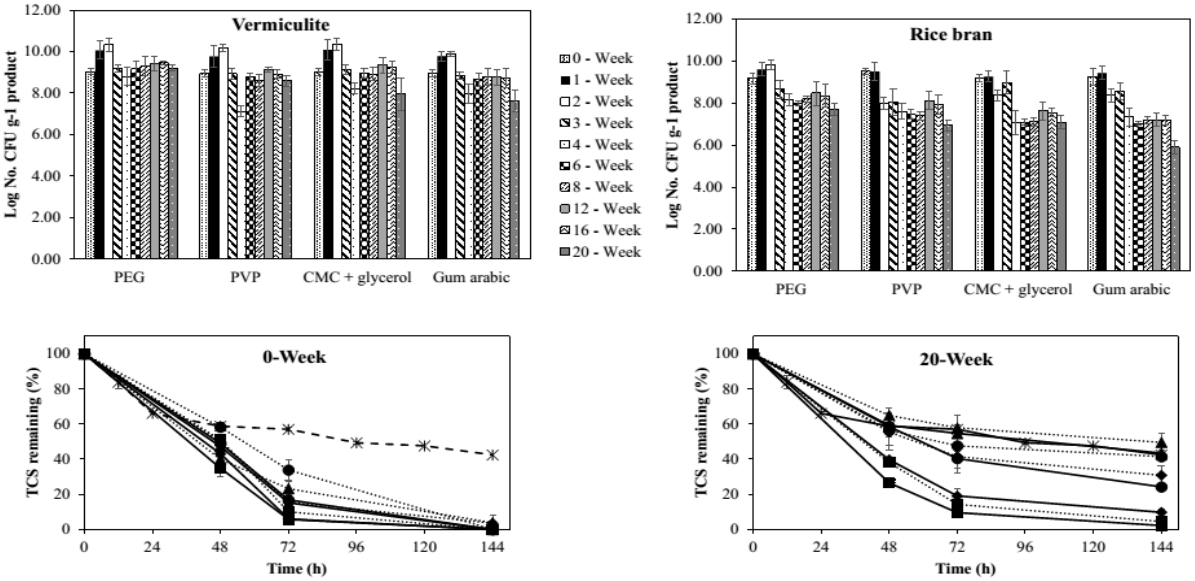

Figure 6. Shelf life of *Pseudomonas* sp. MS45 formulated using vermiculite and rice bran as carrier plus molasses as nutrient and benzoic acid as anti-fungal with different polymer additives (PEG, PVP, CMC+glycerol, and gum arabic) in MSMY plus TCS agar plates; and TCS degradation by formulated *Pseudomonas* sp. MS45 at 0-week and 20-week storage was conducted in MSM liquid medium (B). Vermiculite-PEG (—■—); Vermiculite-PVP (···■···); Vermiculite-CMC + glycerol (—◆—); Vermiculite-Gum Arabic (···◆···); Rice bran-PEG (—●—); Rice bran-PVP (···●···); Rice bran-CMC + glycerol (—▲—); Rice bran-Gum Arabic (···▲···); and before formulation (– ✳ –)

This work investigated the activity of the developed formulations of *Pseudomonas* sp. MS45, at 0-week and 20-week storage, to degrade TCS. The results demonstrated that *Pseudomonas* sp. MS45 in all formulations at 0 weeks exhibited much higher ability in TCS removal than *Pseudomonas* sp. MS45 before formulation, CFU count was much lower (7.12 log CFU mL^{-1}). Almost 40 µM of the initial concentration of TCS was degraded in 144 h. The formulation in vermiculite with PEG was highly effective in deleting TCS because the efficacy was stable at 0-week and 20-week storage. While, *Pseudomonas* sp. MS45 in other formulations showed less ability, especially rice bran with gum arabic.

All the results revealed that the reduction in cell viability reduced the ability of *Pseudomonas* sp. MS45 to degrade TCS. The present study indicates that the formulation of *Pseudomonas* sp. MS45 in vermiculite with PEG is a promising alternative to removing TCS from environmental soils. It is expected to efficiently clean up TCS and develop plant growth in TCS-contaminated agricultural soils.

A previous study demonstrated that inoculating crops with native *Bradyrhizobium* strains prepared with biochar improves soil health and crop growth. However, it is crucial to remember that this kind of inoculation might also have a detrimental effect on other elements of crop development and soil health. Before implementing such immunization programs on a large scale, a substantial study must be conducted to determine the potential risks and benefits (Araujo et al. 2020).

Nonetheless, the findings of this study cannot be generalized to other biopurification systems due to differences in environmental conditions and bacterial communities and in a recent study using a biopurification system made of soil and vermicompost, discovered that environmental conditions and bacterial communities had a great impact on TCS degradation. Environmental conditions and bacterial communities respond differently to TCS due to intrinsic variations (Delgado-Moreno et al. 2021). While using plant-growth-promoting bacteria in soils contaminated with metal can be beneficial, there is also the potential for unintended consequences. One such consequence is the increased uptake of metals by plants, which could lead to toxicity and negatively impact food safety. It is important to carefully evaluate the risks and benefits of using such bacteria in contaminated soils (Gupta et al. 2024).

In concluison, the need for an efficient biological treatment to eliminate such a hazardous substance from soil stems from the discovery of TCS in the soil environment: *Pseudomonas* sp. MS45, a strain that can use TCS as its only carbon and energy source, was isolated and identified in this work by treating *Pseudomonas* sp. MS45, the toxicity of solutions containing TCS is reduced, resulting in a comparatively low ecological risk, according to toxicity tests using *A. cepa* root tips. The PGPB features, which include phosphate-solubilization, Exo-Polysaccharides (EPS), Indole Acetic Acid (IAA), siderophore, ammonia (NH3), and organic acids, are inherited by the isolated TCS-degrading *Pseudomonas* sp. MS45. Moreover, the formulation of *Pseudomonas* sp. MS45, using vermiculite as the basic carrier and PEG as an additive, shows the highest self-life and best efficacy to degrade TCS. Hence, the *Pseudomonas* sp. MS45 has enormous potential to act as a green technology to clean up sites contaminated with TCS.

ACKNOWLEDGEMENTS

During the experiment, the researcher was honored to be supervised by Prof. Alisa Vangnai, Ph.D., from Department of Biochemistry, Chulalongkorn University, Bangkok, Thailand, and funded by Universitas Balikpapan, East Kalimantan, Indonesia.

REFERENCES

Aguilar-Romero I, Romero E, Wittich R-M, van Dillewijn P. 2020. Bacterial ecotoxicity and shifts in bacterial communities associated with the removal of ibuprofen, diclofenac and triclosan in biopurification systems. Sci Total Environ 741: 140461. DOI: 10.1016/j.scitotenv.2020.140461.

Alves ARA, Yin Q, Oliveira RS, Silva EF, Novo LAB. 2022. Plant growth-promoting bacteria in phytoremediation of metal-polluted soils: Current knowledge and future directions. Sci Total Environ 838 (Pt 4): 156435. DOI: 10.1016/j.scitotenv.2022.156435.

Araujo J, Díaz-Alcántara C-A, Urbano B, González-Andrés F. 2020. Inoculation with native *Bradyrhizobium* strains formulated with biochar as carrier improves the performance of pigeonpea (*Cajanus cajan* L.). Eur J Agron 113: 125985. DOI: 10.1016/j.eja.2019.125985.

Araújo MJ, Quintaneiro C, Rocha RJM, Pousão-Ferreira P, Candeias-Mendes A, Soares AMVM, Monteiro MS. 2022. Single and combined effects of ultraviolet radiation and triclosan during the metamorphosis of *Solea senegalensis*. Chemosphere 307 (Pt 1): 135583. DOI: 10.1016/j.chemosphere.2022.135583.

Balakrishnan P, Mohan S. 2021. Treatment of triclosan through enhanced microbial biodegradation. J Hazard Mater 420: 126430. DOI: 10.1016/j.jhazmat.2021.126430.

Blanco-Vargas A, Rodríguez-Gacha LM, Sánchez-Castro N, Garzón-Jaramillo R, Pedroza-Camacho LD, Poutou-Piñales RA, Rivera-Hoyos CM, Díaz-Ariza LA, Pedroza-Rodríguez AM. 2020. Phosphate-solubilizing *Pseudomonas* sp., and *Serratia* sp., co-culture for *Allium cepa* L. growth promotion. Heliyon 6 (10): e05218. DOI: 10.1016/j.heliyon.2020.e05218.

Chan SS, Khoo KS, Chew KW, Ling TC, Show PL. 2022. Recent advances biodegradation and biosorption of organic compounds from wastewater: Microalgae-bacteria consortium-A review. Bioresour Technol 344: 126159. DOI: 10.1016/j.biortech.2021.126159.

Chen Y, Chen Y, Jia J, Yan B. 2022. Triclosan detoxification through dechlorination and oxidation via microbial Pd-NPs under aerobic conditions. Chemosphere 286 (Pt 3): 131836. DOI: 10.1016/j.chemosphere.2021.131836.

Chen J, Zhang B, Wang C, Wang P, Cui G, Gao H, Feng B, Zhang J. 2024. Insight into the enhancement effect of humic acid on microbial degradation of triclosan in anaerobic sediments. J Hazard Mater 461: 132549. DOI: 10.1016/j.jhazmat.2023.132549.

Contardo-Jara V, Meinecke S, Feibicke M, Berghahn R, Schmidt R, Mohr S. 2021. Fate, bioaccumulation and toxic effects of triclosan on a freshwater community-A mesocosm study. Environ Adv 5: 100100. DOI: 10.1016/j.envadv.2021.100100.

Cruz JA, Tubana BS, Fultz LM, Dalen MS, Ham JH. 2022. Identification and profiling of silicate-solubilizing bacteria for plant growth-promoting traits and rhizosphere competence. Rhizosphere 23: 100566. DOI: 10.1016/j.rhisph.2022.100566.

Cui K, Xu T, Chen J, Yang H, Liu X, Zhuo R, Peng Y, Tang W, Wang R, Chen L, Zhang X, Zhang Z, He Z, Wang X, Liu C, Chen Y, Zhu Y. 2022. Siderophores, a potential phosphate solubilizer from the endophyte *Streptomyces* sp. CoT10, improved phosphorus mobilization for host plant growth and rhizosphere modulation. J Clean Prod 367: 133110. DOI: 10.1016/j.jclepro.2022.133110.

Dai H, Gao J, Wang S, Li D, Wang Z. 2020. The key active degrader, metabolic pathway and microbial ecology of triclosan biodegradation in an anoxic/oxic system. Bioresour Technol 317: 124014. DOI: 10.1016/j.biortech.2020.124014.

Dai H, Gao J, Li D, Wang Z, Cui Y, Zhao Y. 2022a. Family Sphingomonadaceae as the key executor of triclosan degradation in both nitrification and denitrification systems. Chem Eng J 442: 136202. DOI: 10.1016/j.cej.2022.136202.

Dai H, Gao J, Li D, Wang Z, Duan W. 2022b. DNA-based stable isotope probing deciphered the active denitrifying bacteria and triclosan-degrading bacteria participating in granule-based partial denitrification process under triclosan pressure. Water Res 210: 118011. DOI: 10.1016/j.watres.2021.118011.

Dayamani KJ, Brahmaprakash GP. 2014. Influence of form and concentration of the osmolytes in liquid inoculants formulations of plant growth promoting bacteria. Intl J Sci Res Publ 4 (7): 449-454.

Delgado-Moreno L, van Dillewijn P, Nogales R, Romero E. 2021. Straw-based biopurification systems to remove ibuprofen, diclofenac and triclosan from wastewaters: Dominant microbial communities. Agronomy 11 (8): 1507. DOI: 10.3390/agronomy11081507.

Devatha CP, Pavithra N. 2019. Isolation and identification of *Pseudomonas* from wastewater, its immobilization in cellulose biopolymer and performance in degrading triclosan. J Environ Manag 232: 584-591. DOI: 10.1016/j.jenvman.2018.11.083.

Dong X, He Y, Peng X, Jia X. 2021. Triclosan in contact with activated sludge and its impact on phosphate removal and microbial community. Bioresour Technol 319: 124134. DOI: 10.1016/j.biortech.2020.124134.

Dou R-N, Wang J-H, Chen Y-C, Hu Y-Y. 2018. The transformation of triclosan by laccase: Effect of humic acid on the reaction kinetics, products and pathway. Environ Pollut 234: 88-95. DOI: 10.1016/j.envpol.2017.10.119.

Durán-Álvarez JC, Prado B, González D, Sánchez Y, Jiménez-Cisneros B. 2015. Environmental fate of naproxen, carbamazepine and triclosan in wastewater, surface water and wastewater irrigated soil - results of laboratory scale experiments. Sci Total Environ 538: 350-362. DOI: 10.1016/j.scitotenv.2015.08.028.

Fitriatin BN, Jingga A, Kamaluddin NN, Setiawati MR, Simarmata T. 2022. Characterization and bioassay of rhizophosphate bacteria producing phytohormone and organic acid to enhance the maize seedling growth. Polish J Soil Sci 55 (2): 93-104. DOI: 10.17951/pjss.2022.55.2.93-104.

Franke S, Seidel K, Adrian L, Nijenhuis I. 2020. Dual element (C/Cl) isotope analysis indicates distinct mechanisms of reductive dehalogenation of chlorinated ethenes and dichloroethane in *Dehalococcoides mccartyi* strain BTF08 with defined reductive dehalogenase inventories. Front Microbiol 11: 1507. DOI: 10.3389/fmicb.2020.01507.

Gopalakrishnan S, Sathya A, Vijayabharathi R, Srinivas V. 2016. Formulations of plant growth-promoting microbes for field applications. In: Singh DP, Singh HB, Prabha R (eds). Microbial Inoculants in Sustainable Agricultural Productivity. Springer, New Delhi. DOI: 10.1007/978-81-322-2644-4_15.

Goswami D, Dhandhukia P, Patel P, Thakker JN. 2014. Screening of PGPR from saline desert of Kutch: Growth promotion in *Arachis hypogea* by *Bacillus licheniformis* A2?. Microbiol Res 169 (1): 66-75. DOI: 10.1016/j.micres.2013.07.004.

Granatto CF, Grosseli GM, Sakamoto IK, Fadini PS, Varesche MBA. 2021. Influence of metabolic co-substrates on methanogenic potential and degradation of triclosan and propranolol in sanitary sewage. Environ Res 199: 111220. DOI: 10.1016/j.envres.2021.111220.

Gupta R, Khan F, Alqahtani FM, Hashem M, Ahmad F. 2024. Plant Growth-Promoting Rhizobacteria (PGPR) assisted bioremediation of heavy metal toxicity. Appl Biochem Biotechnol 196 (5): 2928-2956. DOI: 10.1007/s12010-023-04545-3.

Hajieghrari M, Hejazi P. 2020. Enhanced biodegradation of n-Hexadecane in solid-phase of soil by employing immobilized *Pseudomonas aeruginosa* on size-optimized coconut fibers. J Hazard Mater 389: 122134. DOI: 10.1016/j.jhazmat.2020.122134.

Haq I, Raj A, Markandeya. 2018. Biodegradation of Azure-B dye by *Serratia liquefaciens* and its validation by phytotoxicity, genotoxicity and cytotoxicity studies. Chemosphere 196: 58-68. DOI: 10.1016/j.chemosphere.2017.12.153.

He Z, Honeycutt CW. 2005. A modified molybdenum blue method for orthophosphate determination suitable for investigating enzymatic hydrolysis of organic phosphates. Commun Soil Sci Plant Anal 36 (9-10): 1373-1383. DOI: 10.1081/CSS-200056954.

Hirsch PR, Mauchline TH. 2015. The importance of the microbial N cycle in soil for crop plant nutrition. Adv Appl Microbiol 93: 45-71. DOI: 10.1016/bs.aambs.2015.09.001.

Holkar CR, Pandit AB, Pinjari DV. 2014. Kinetics of biological decolorisation of anthraquinone based reactive blue 19 using an isolated strain of *Enterobacter* sp. F NCIM 5545. Bioresour Technol 173: 342-351. DOI: 10.1016/j.biortech.2014.09.108.

Jayalatha NA, Devatha CP. 2023. Experimental investigation for treating ibuprofen and triclosan by biosurfactant from domestic wastewater. J Environ Manag 328: 116913. DOI: 10.1016/j.jenvman.2022.116913.

Kumar V, Ameen F, Islam MA, Agrawal S, Motghare A, Dey A, Shah MP, Américo-Pinheiro JHP, Singh S, Ramamurthy PC. 2022. Evaluation of cytotoxicity and genotoxicity effects of refractory pollutants of untreated and biomethanated distillery effluent using *Allium cepa*. Environ Pollut 300: 118975. DOI: 10.1016/j.envpol.2022.118975.

Li Q, Yu J, Chen W, Ma X, Li G, Chen G, Deng J. 2018. Degradation of triclosan by chlorine dioxide: Reaction mechanism, 2, 4-dichlorophenol accumulation and toxicity evaluation. Chemosphere 207: 449-456. DOI: 10.1016/j.chemosphere.2018.05.065.

Ma C, Hua J, Li H, Zhang J, Luo S. 2022. Inoculation with carbofuran-degrading rhizobacteria promotes maize growth through production of IAA and regulation of the release of plant-specialized metabolites. Chemosphere 307: 136027. DOI: 10.1016/j.chemosphere.2022.136027.

Maheshwari DK, Dubey RC, Agarwal M, Dheeman S, Aeron A, Bajpai VK. 2015. Carrier based formulations of biocoenotic consortia of disease suppressive *Pseudomonas aeruginosa* KRP1 and *Bacillus licheniformis* KRB1. Ecol Eng 81: 272-277. DOI: 10.1016/j.ecoleng.2015.04.066.

Mallak AM, Lakzian A, Khodaverdi E, Haghnia GH, Mahmoudi S. 2020. Effect of *Pleurotus ostreatus* and *Trametes versicolor* on triclosan biodegradation and activity of laccase and manganese peroxidase enzymes. Microb Pathog 149: 104473. DOI: 10.1016/j.micpath.2020.104473.

McPherson MR, Wang P, Marsh EL, Mitchell RB, Schachtman DP. 2018. Isolation and analysis of microbial communities in soil, rhizosphere, and roots in perennial grass experiments. J Vis Exp 137: e57932. DOI: 10.3791/57932.

Nandikes G, Pathak P, Abd Razak AS, Narayanamurthy V, Singh L. 2022. Occurrence, environmental risks and biological remediation mechanisms of triclosan in wastewaters: Challenges and perspectives. J Water Proc Eng 49: 103078. DOI: 10.1016/j.jwpe.2022.103078.

Nandikes G, Pathak P, Singh L. 2024. Unveiling microbial degradation of triclosan: Degradation mechanism, pathways, and catalyzing clean energy. Chemosphere 357: 142053. DOI: 10.1016/j.chemosphere.2024.142053.

Naseem H, Ahsan M, Shahid MA, Khan N. 2018. Exopolysaccharides producing rhizobacteria and their role in plant growth and drought tolerance. J Basic Microbiol 58 (12): 1009-1022. DOI: 10.1002/jobm.201800309.

Nie E, Wang H, Chen Y, Lu Y, Akhtar K, Riaz M, Zhang S, Yu Z, Ye Q. 2022. Distinct uptake and accumulation profiles of triclosan in youdonger (*Brassica campestris* subsp. *chinensis* var. *communis*) under two planting systems: Evidence from 14C tracing techniques. Chemosphere 288: 132651. DOI: 10.1016/j.chemosphere.2021.132651.

Olanrewaju OS, Glick BR, Babalola OO. 2017. Mechanisms of action of plant growth promoting bacteria. World J Microbiol Biotechnol 33 (11): 197. DOI: 10.1007/s11274-017-2364-9.

Olaniyan LWB, Mkwetshana N, Okoh AI. 2016. Triclosan in water, implications for human and environmental health. SpringerPlus 5: 1639. DOI: 10.1186/s40064-016-3287-x.

Pan Y, Zheng X, Xiang Y. 2021. Structure-function elucidation of a microbial consortium in degrading rice straw and producing acetic and butyric acids via metagenome combining 16S rDNA sequencing. Bioresour Technol 340: 125709. DOI: 10.1016/j.biortech.2021.125709.

Pacwa-Płociniczak M, Płociniczak T, Iwan J, Żarska M, Chorążewski M, Dzida M, Piotrowska-Seget Z. 2016. Isolation of hydrocarbon-degrading and biosurfactant-producing bacteria and assessment their plant growth-promoting traits. J Environ Manag 168: 175-184. DOI: 10.1016/j.jenvman.2015.11.058.

Phulpoto IA, Yu Z, Li J, Ndayisenga F, Hu B, Qazi MA, Yang X. 2022. Evaluation of di-rhamnolipid biosurfactants production by a novel *Pseudomonas* sp. S1WB: Optimization, characterization and effect on petroleum-hydrocarbon degradation. Ecotoxicol Environ Saf 242: 113892. DOI: 10.1016/j.ecoenv.2022.113892.

Qi X, Wang H, Gao X, Zhang L, Wang S, Wang X, Xu P. 2022. Efficient power recovery from aromatic compounds by a novel electroactive bacterium *Pseudomonas putida* B6-2 in microbial fuel cells. J Environ Chem Eng 10 (6): 108536. DOI: 10.1016/j.jece.2022.108536.

Qu S, Shen C, Zhang L, Wang J, Zhang L-M, Chen B, Sun G-X, Ge Y. 2023. Dispersal limitation and host selection drive geo-specific and plant-specific differentiation of soil bacterial communities in the Tibetan alpine ecosystem. Sci Total Environ 863: 160944. DOI: 10.1016/j.scitotenv.2022.160944.

Reeves MW, Pine L, Neilands JB, Balows A. 1983. Absence of siderophore activity in *Legionella* species grown in iron-deficient media. J Bacteriol 154 (1): 324-329. DOI: 10.1128/jb.154.1.324-329.1983.

Satapute P, Paidi MK, Kurjogi M, Jogaiah S. 2019. Physiological adaptation and spectral annotation of arsenic and cadmium heavy metal-resistant and susceptible strain *Pseudomonas taiwanensis*. Environ Pollut 251: 555-563. DOI: 10.1016/j.envpol.2019.05.054.

Schlatter DC, Gamble JD, Castle S, Rogers J, Wilson M. 2022. Abiotic and biotic filters determine the response of soil bacterial communities to manure amendment. Appl Soil Ecol 180: 104618. DOI: 10.1016/j.apsoil.2022.104618.

Scussel R, Feltrin AC, Angioletto E, Galvani NC, Fagundes MÍ, Bernardin AM, Feuser PE, de Ávila RAM, Pich CT. 2022. Ecotoxic, genotoxic, and cytotoxic potential of leachate obtained from chromated copper arsenate-treated wood ashes. Environ Sci Pollut Res 29 (27): 41247-41260. DOI: 10.1007/s11356-021-18413-2.

Shah Z, Gulzar M, Hasan F, Shah AA. 2016. Degradation of polyester polyurethane by an indigenously developed consortium of *Pseudomonas* and *Bacillus* species isolated from soil. Polym Degrad Stab 134: 349-356. DOI: 10.1016/j.polymdegradstab.2016.11.003.

Sharma A, Vázquez LAB, Hernández EOM, Becerril MYM, Oza G, Ahmed SSSJ, Ramalingam S, Iqbal HMN. 2022a. Green remediation potential of immobilized oxidoreductases to treat halo-organic pollutants persist in wastewater and soil matrices-A way forward. Chemosphere 290: 133305. DOI: 10.1016/j.chemosphere.2021.133305.

Sharma B, Tiwari S, Kumawat KC, Cardinale M. 2022b. Nano-biofertilizers as bio-emerging strategies for sustainable agriculture development: Potentiality and their limitations. Sci Total Environ 860: 160476. DOI: 10.1016/j.scitotenv.2022.160476.

Silambarasan S, Vangnai AS. 2016. Biodegradation of 4-nitroaniline by plant-growth promoting *Acinetobacter* sp. AVLB2 and toxicological analysis of its biodegradation metabolites. J Hazard Mater 302: 426-436. DOI: 10.1016/j.jhazmat.2015.10.010.

Silva VP, Pereira OG, Leandro ES, Da Silva TC, Ribeiro KG, Mantovani HC, Santos SA. 2016. Effects of lactic acid bacteria with bacteriocinogenic potential on the fermentation profile and chemical composition of alfalfa silage in tropical conditions. J Dairy Sci 99 (3) 1895-1902. DOI: 10.3168/jds.2015-9792.

Sindhu SS, Phour M, Choudhary SR, Chaudhary D. 2014. Phosphorus cycling: Prospects of using rhizosphere microorganisms for improving phosphorus nutrition of plants. In: Parmar N, Singh A (eds). Geomicrobiology and Biogeochemistry Springer, Berlin, Heidelberg. DOI: 10.1007/978-3-642-41837-2_11.

Singh R, Arora NK. 2023. Bacterial formulations and delivery systems against pests in sustainable agro-food production. In: Ferranti P (eds). Sustainable Food Science-A Comprehensive Approach. Elsevier Science Publishing Co Inc, India. DOI: 10.1016/B978-0-12-823960-5.00064-0.

Singh VK, Singh AK, Singh PP, Kumar A. 2018. Interaction of plant growth promoting bacteria with tomato under abiotic stress: A review. Agric Ecosyst Environ 267: 129-140. DOI: 10.1016/j.agee.2018.08.020.

Sipahutar MK, Piapukiew J, Vangnai AS. 2018. Efficiency of the formulated plant-growth promoting *Pseudomonas fluorescens* MC46 inoculant on triclocarban treatment in soil and its effect on *Vigna radiata* growth and soil enzyme activities. J Hazard Mater 344: 883-892. DOI: 10.1016/j.jhazmat.2017.11.046.

Sipahutar MK, Vangnai AS. 2017. Role of plant growth-promoting *Ochrobactrum* sp. MC22 on triclocarban degradation and toxicity mitigation to legume plants. J Hazard Mater 329: 38-48. DOI: 10.1016/j.jhazmat.2017.01.020.

Soni RK, Bhatt NS, Modi HA, Acharya PB. 2016. Decolorization, degradation and subsequent toxicity assessment of reactive Red 35 by *Enterococcus qallinarum*. Curr Biotechnol 5 (2): 1-12. DOI: 10.2174/2211550105666151211195703.

Subba Reddy GV, Rafi MM, Rubesh Kumar S, Khayalethu N, Muralidhara Rao D, Manjunatha B, Philip GH, Reddy BR. 2016. Optimization study of 2-hydroxyquinoxaline (2-HQ) biodegradation by *Ochrobactrum* sp. HQ1. 3 Biotech 6: 51. DOI: 10.1007/s13205-015-0358-6.

Sun C, Zhang T, Zhou Y, Liu Z-F, Zhang Y, Bian Y, Feng X-S. 2023. Triclosan and related compounds in the environment: Recent updates on sources, fates, distribution, analytical extraction, analysis, and removal techniques. Sci Total Environ 870: 161885. DOI: 10.1016/j.scitotenv.2023.161885.

Sun W, Alexander T, Man Z, Xiao F, Cui, F, Qi X. 2018. Enhancing 2-ketogluconate production of *Pseudomonas plecoglossicida* JUIM01 by maintaining the carbon catabolite repression of 2-ketogluconate metabolism. Molecules 23: 2629. DOI: 10.3390/molecules23102629.

Suthar S, Chand N, Singh V. 2023. Fate and toxicity of triclosan in tidal flow constructed wetlands amended with cow dung biochar. Chemosphere 311: 136875. DOI: 10.1016/j.chemosphere.2022.136875.

Taştan BE, Tekinay T, Çelik HS, Özdemir C, Cakir DN. 2017. Toxicity assessment of pesticide triclosan by aquatic organisms and degradation studies. Regul Toxicol Pharmacol 91: 208-215. DOI: 10.1016/j.yrtph.2017.10.030.

Thelusmond J-R, Strathmann TJ, Cupples AM. 2019. Carbamazepine, triclocarban and triclosan biodegradation and the phylotypes and functional genes associated with xenobiotic degradation in four agricultural soils. Sci Total Environ 657: 1138-1149. DOI: 10.1016/j.scitotenv.2018.12.145.

Vocciante M, Grifoni M, Fusini D, Petruzzelli G, Franchi E. 2022. The role of Plant Growth-Promoting Rhizobacteria (PGPR) in mitigating plant's environmental stresses. Appl Sci 12 (3): 1231. DOI: 10.3390/app12031231.

Wang S, Yin Y, Wang J. 2017. Enhanced biodegradation of triclosan by means of gamma irradiation. Chemosphere 167: 406-414. DOI: 10.1016/j.chemosphere.2016.10.028.

Yadav A, Raj A, Purchase D, Ferreira LFR, Saratale GD, Bharagava RN. 2019. Phytotoxicity, cytotoxicity and genotoxicity evaluation of organic and inorganic pollutants rich tannery wastewater from a Common Effluent Treatment Plant (CETP) in Unnao district, India using *Vigna radiata* and *Allium cepa*. Chemosphere 224: 324-332. DOI: 10.1016/j.chemosphere.2019.02.124.